

# Ultra-wide band gap metasurfaces for controlling seismic surface waves

Wenlong Liu<sup>a,b,1</sup>, Gil Ho Yoon<sup>b,\*,1</sup>, Bing Yi<sup>a,\*,1</sup>, Yue Yang<sup>a,c,1</sup>, Yi Chen<sup>a,1</sup>

<sup>a</sup> School of Traffic and Transportation Engineering, Central South University, Changsha, China

<sup>b</sup> School of Mechanical Engineering, Hanyang University, Seoul, South Korea

<sup>c</sup> CRRC ZHUZHOU LOCOMOTIVE CO.,LTD., Zhuzhou, China



## ARTICLE INFO

### Article history:

Received 1 July 2020

Received in revised form 9 September 2020

Accepted 28 September 2020

Available online 30 September 2020

### Keywords:

Metasurface

Ultra-wide band gap

Seismic surface waves

Metabridge

## ABSTRACT

Metamaterials have been widely studied for their advantage in the effective control of the propagation of mechanical waves. However, existing methods are limited in controlling the propagation of seismic surface waves and hardly are put in practical engineering applications. To overcome this limitation, we introduce a new type of metasurface with ultra-wide band gaps for controlling the seismic surface waves, which can be further applied to engineering applications. The metasurface is designed by using an easy and simple method named the destructive interference, rather than the local resonance observed in previous methods. Furthermore, the designed unit structure can construct a periodic structure by using the functional gradient design and combination arrangement, which results in hitherto better or even unprecedented performance in controlling the propagation of seismic surface waves. Moreover, the proposed metasurface provides new opportunities for practical engineering applications, as demonstrated by the metabridge can effectively protect the bridge from the damage of earthquakes.

© 2020 Elsevier Ltd. All rights reserved.

## 1. Introduction

To reduce structural damage and ensure personal safety, the engineering community is constantly looking for cutting-edge technology to control the adverse effects caused by seismic surface waves. This research topic has been widely concerned recently, as the increase of seismic sources that can generate seismic surface waves, for example, but not limited to earthquakes, pile driving in civil engineering and railway trains. To overcome this problem, several methods have been developed, of which the metamaterial opened up a new area for controlling the propagation of seismic surface waves [1–3]. Metamaterials are artificial engineering materials that derive their properties from structure rather than composition, which exhibit auxetic physical performance that hardly can be found in most natural materials, such as the phononic crystal which prohibits the propagation of mechanical waves [4–7]. Inspired by the previous work on phononic crystal, a recently emerging soil-metamaterials was developed to control the propagation of seismic surface waves, which insert structured soil made of cylindrical voids or rigid inclusions into the soil according to a predestinate arrangement,

thereby creating a phononic crystal with a band gap. A detailed description of the soil-metamaterials can be found in [8,9] and references therein, recent related researches can be found in [10–14]. Although soil-metamaterials can control the propagation of seismic surface waves, further applications are limited due to the following shortcomings: (1) narrowband is their common characteristic, and (2) the inserted inclusions will destroy the soil geology and cause hidden collateral damage.

On the other hand, the metasurfaces have received extensive attention due to its auxetic physical performance of manipulating the wavefront [15]. Recently, metasurfaces with some new properties have been developed and used in engineering applications, such as planar hologram [16], vortex generator [17], and beam deflector [18], and also some other advances [19–23]. Here, focus on the progress of the metasurfaces in controlling seismic surface waves. Metasurfaces are studied for manipulating the propagation of surface waves [24–27], and large geophysical experiments demonstrate that natural forest trees can be used as metasurfaces [28,29]. Similar methods using metasurfaces for manipulating surface waves can be found in [30,31]. However, the existing methods are limited in controlling the propagation of seismic surface waves for that a structure with low-frequency and wide band gaps are required for practical engineering applications. Therefore, it is necessary to explore new mechanisms and approaches to cope with this challenge.

Hence, we introduce a new type of metasurface with ultra-wide band gaps for controlling the seismic surface waves, which

\* Corresponding authors.

E-mail addresses: [ghy@hanyang.ac.kr](mailto:ghy@hanyang.ac.kr) (G.H. Yoon), [bingyi@csu.edu.cn](mailto:bingyi@csu.edu.cn) (B. Yi).

<sup>1</sup> All authors contributed equally.

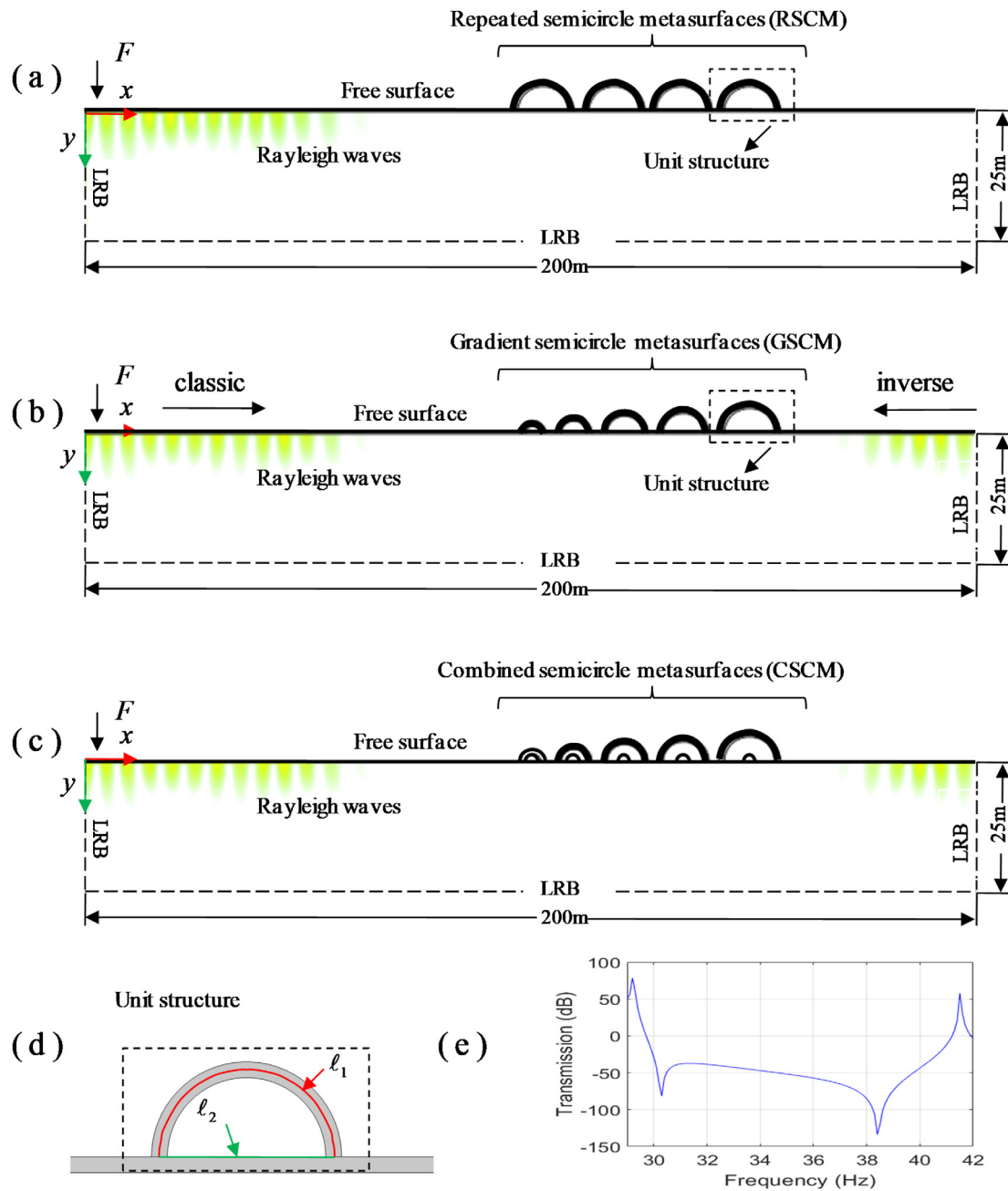


**Fig. 1.** Seismic metasurfaces design and unit structure properties, (a) Repeated semicircle metasurfaces. (b) Gradient semicircle metasurfaces. (c) Combined semicircle metasurfaces. (d) unit structure. (e) The band gap characteristic of the unit structure.

can be further applied to engineering applications. The metasurface is designed by using an easy and simple method named the destructive interference, rather than the local resonance observed in previous methods. We demonstrate the design of the periodic structure with a simple unit structure by using the functional gradient design and combination arrangement methods, which results in hitherto better or even unprecedented performance in controlling the propagation of seismic surface waves. Moreover, we also show that the proposed metasurface provides new opportunities for practical engineering applications, as demonstrated by the proposed metabridge can effectively protect the bridge from the damage of earthquakes.

## 2. Design of the metasurfaces for controlling seismic surface waves

### 2.1. Metasurfaces and unit structure properties

A conceptual illustration of the proposed metasurface is shown in Fig. 1a–c, and the figure inset shows the unit structure (Fig. 1d) that can be independently designed to control wave propagation. More precisely, the band gap characteristic of the unit structure can control the wave propagation in a specific frequency range, and the theoretical method for achieving a band gap characteristic is the destructive interference. Here, in terms of the unit structure, the mathematical expression of destructive

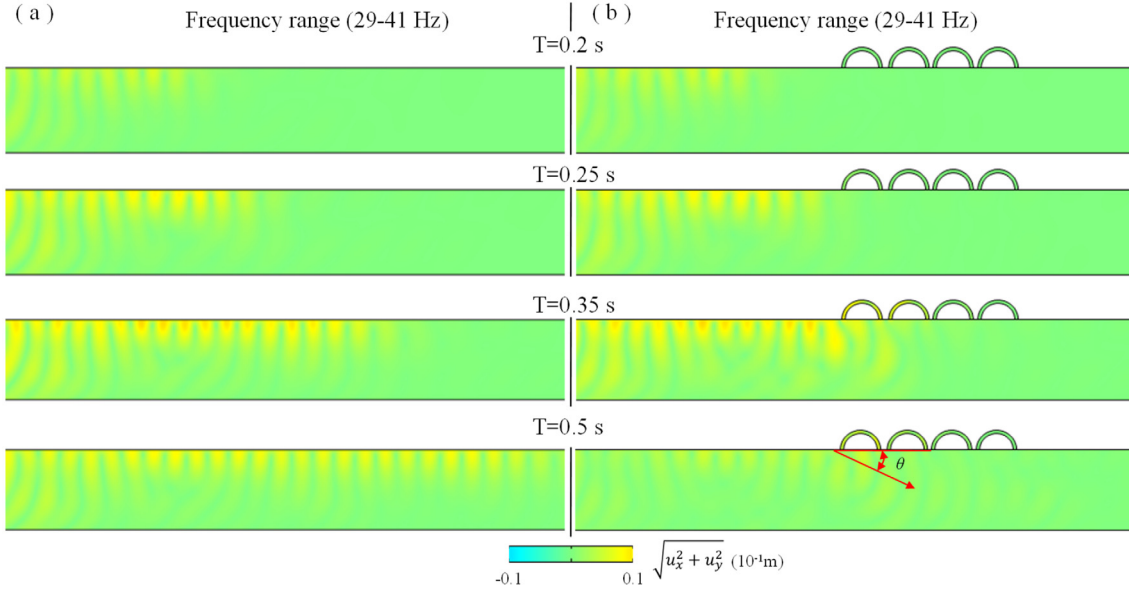


Fig. 2. Snapshots of Rayleigh wave propagating at different times, (a) without and (b) with repeated semicircle metasurfaces.

interference is defined as

$$\delta = \ell_1 - \ell_2 = (k + 1/2)\lambda, k = 0, 1, 2, \dots \quad (1)$$

where,  $\ell_1$  and  $\ell_2$  are long and short sides of the unit structure, as shown in Fig. 1d,  $\lambda$  is the wavelength that satisfies the relationship  $c = \lambda \cdot f$ ,  $c$  is the wave speed propagating in structure. Here, to illustrate the band gap characteristics of the unit structure, we take the shear wave as an example, and the wave speed  $c_s = \sqrt{E/[2(1 + \mu)\rho]}$ , where  $E$ ,  $\mu$ , and  $\rho$  are elastic modulus, Poisson's ratio, and density of unit structure, respectively. Based on the mechanism described in Eq. (1), a unit semicircle structure was designed with  $\ell_2 = 6$  m,  $\ell_1 = \pi\ell_2/2 = 9.42$  m, and the thickness is 1 m. By performing finite element analysis using the COMSOL Multiphysics package, the band gap characteristic of the unit semicircle structure was obtained, as shown in Fig. 1e. Details on the design and characteristics of the unit structure can be found in Supplementary Note 1 and Fig. 1. According to the steps of the proposed method, readers can design and combine different unit structures to obtain metamaterials with different application requirements. In the present work, utilizing the unit structure shown in Fig. 1d, three types of metasurfaces for controlling the propagation of Rayleigh waves can be designed. Among them, the RSCM is a simple periodic arrangement of the unit structure, as shown in Fig. 1a. The GSCM (Fig. 1b) is a gradient semicircular metasurface composed of unit structures with different sizes, which are to obtain different  $\delta$ , that is, to obtain band gaps ranging in different frequencies which satisfies Eq. (1). In addition, the varying way in CSCM (Fig. 1c) is to combine the GSCM presented in this paper and the RSCM composed of the unit structure which scaled by 0.4 times.

## 2.2. Mode-conversion characteristics of the proposed metasurface

As mentioned in the previous methods [24,28,32], metasurfaces can exhibit mode-conversion characteristics for controlling the propagation of surface waves, i.e., the ability to convert surface waves into a harmless shear wave. Moreover, the downward propagation angle satisfies generalized Snell's law [15], as follows.

$$\sin(\theta_t)n_t - \sin(\theta_i)n_i = \frac{\lambda_o}{2\pi} \frac{d\phi}{dx} \quad (2)$$

where  $\theta_t$  is the angle of refraction, and  $\theta_i$  is the angle between the incident wave and the normal plane of the propagation medium;

$n_i$  and  $n_t$  are the refractive indices of the two media;  $\lambda_o$  is the vacuum wavelength and  $\phi$  is the position where the incident wave crosses the medium plane. In this paper, considering that the Rayleigh wave and shear wave propagate in the same medium, i.e., earth, we can obtain  $n_i = c/c_R$ ,  $n_t = c/c_s$ , and  $\theta_i = 90^\circ$ ,  $d\phi/dx = 0$ , as shown in the following Fig. 1. In short, combined with wave propagation conditions in this paper, Eq (2) can be transformed into  $\sin(\theta_t) = c_s/c_R$ , therefore the downward propagation angle  $\theta = 90^\circ - \arcsin(c_s/c_R)$ .

In the following, to demonstrate the mode-conversion characteristics of the proposed metasurface, the finite element analysis was conducted on the 2D half-space model of the RSCM and GSCM. Throughout the paper, the finite element analysis was performed using finite element software COMSOL Multiphysics, and the simulation frequency used in Figs. 2–5 is the central frequency of the band gap range for the unit structure, that is, the central frequency of the range marked in each figure. All simulations were conducted on the 2D half-space model. The specific settings are as follows: As shown in Fig. 1a–c, where  $F$  is a force along the  $y$ -direction, which simulates a source that produces Rayleigh wave and using  $F = 1e^6 \cdot \sin(2\pi f_0 t)$ . The ground properties in 2D half-space are characterized by a homogeneous material, that is, ground properties:  $v_p = 900$  m/s,  $v_s = 500$  m/s, and  $\rho = 1200$  kg/m<sup>3</sup>, a similar method for simulating ground properties can be found in Refs. [24,28]. As for the material of the unit semicircle structure, we select the concrete material with  $\rho = 2300$  kg/m<sup>3</sup>,  $E = 25$  GPa,  $n_u = 0.2$ , which is the built-in material of software COMSOL Multiphysics. Besides, to reduce the influence of reflected waves on the analysis results, the bottom and vertical boundaries are set as low reflection boundaries (LRB). Furthermore, to better show the Rayleigh wave propagation process, the mesh settings for finite element analysis are defined as the minimum mesh element size, i.e.,  $r_{min} = c_R/f_{max}$ , where  $f_{max}$  is the maximum frequency of the controllable Rayleigh waves. The snapshots of Rayleigh waves propagating at different times are shown in Figs. 2–4.

In Fig. 2, we show the numerical results demonstrating the mode-conversion characteristics of the RSCM. Remarkably, one can find that the RSCM exhibits the ability to control the propagation of Rayleigh waves. More importantly, as shown in the snapshot of  $T = 0.5$  s in Fig. 2b, the propagating Rayleigh wave is converted into a shear wave with a downward refraction angle of

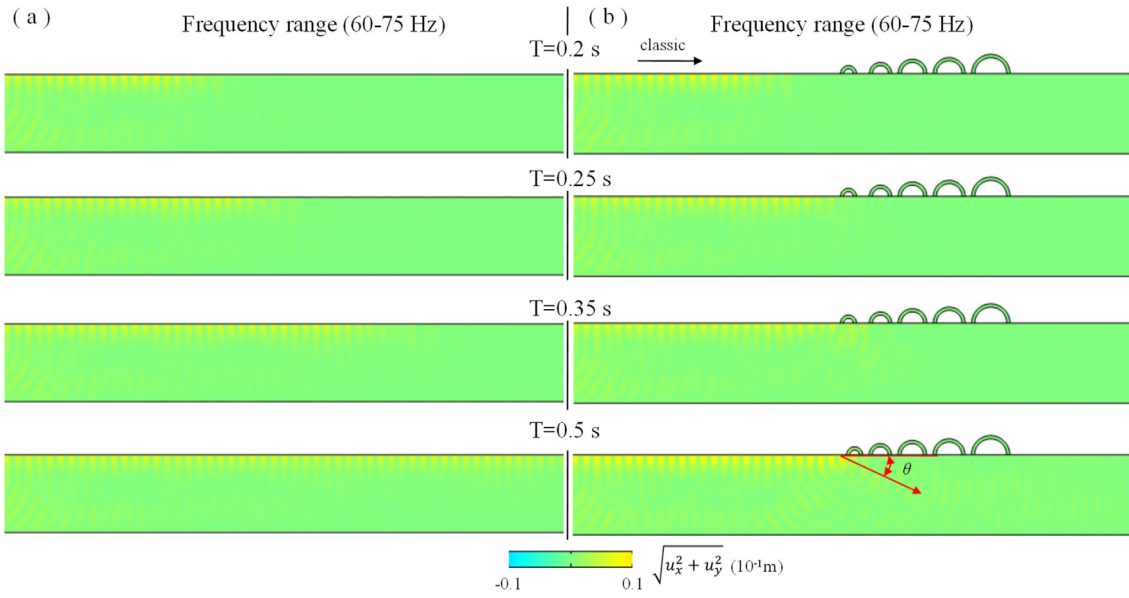


Fig. 3. Snapshots of Rayleigh wave propagating at different times, (a) without and (b) with gradient semicircle metasurfaces (classic metasurfaces).

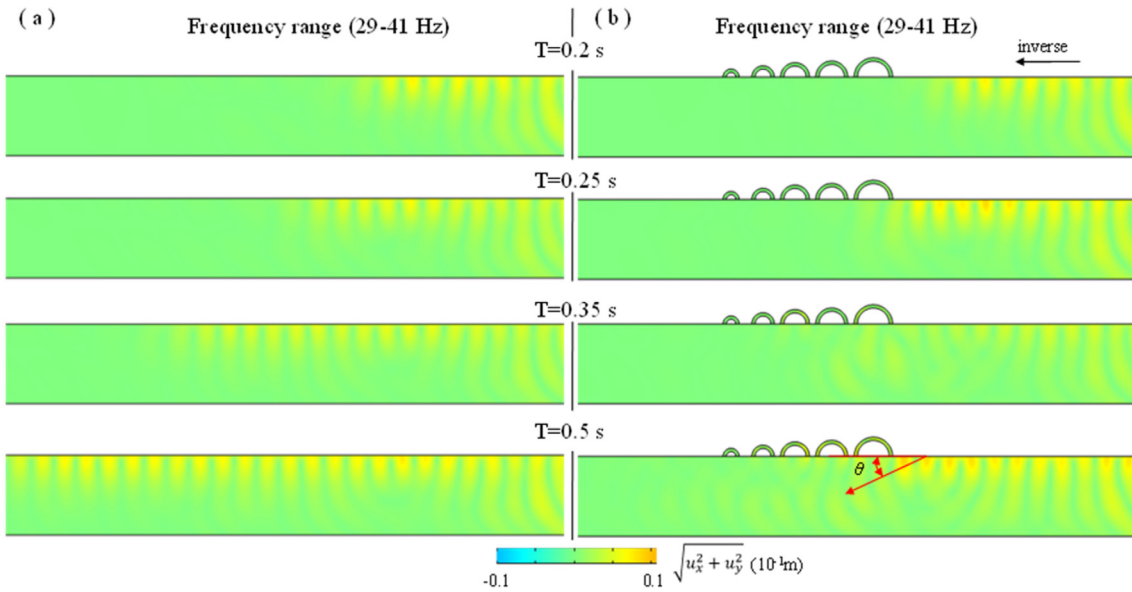


Fig. 4. Snapshots of Rayleigh wave propagating at different times, (a) without and (b) with gradient semicircle metasurfaces (inverse metasurfaces).

$\sim 25^\circ$ , which is consistent with the modal-conversion characteristics described in [24], here, the dynamic numerical results see Supplementary Fig. 2. On the other hand, the numerical results of mode-conversion characteristics exhibited by GSCM are shown in Figs. 3 and 4, which correspond to the two types of incident waves entering the GSCM, namely the classic metasurface and inverse metasurface. As shown in Figs. 3 and 4, for both types of incident waves, GSCM shows the mode-conversion characteristics for controlling the propagation of Rayleigh waves. It should be noted that the frequency ranges marked in Figs. 2–4 are the band gap frequency ranges of the first unit structure in the proposed metasurface, which is located in the direction of the incident waves. The dynamic results of Rayleigh wave propagation in the full frequency range see Supplementary Fig. 3, Fig. 4, and Fig. 5. Another thing to note here is that the incident wave frequency is

not within band gap frequency ranges of the first unit structure in GSCM, but within that of GSCM, GSCM can exhibit the “seismic rainbow” as described in [28], as shown in Fig. 5.

### 2.3. Metasurfaces for ultra-wide band gap

As described above, controlling the adverse effects caused by seismic surface waves has been widely concerned in recent years. However, to the best of our knowledge, existing methods cannot simultaneously take into account the performance requirements of low-frequency and wide band gap. To address this issue, we design and numerically demonstrate that CSCM exhibits unprecedented performance in both low-frequency and ultra-wide band gap for controlling the propagation of Rayleigh waves. However, before the numerical verification of the designed CSCM exhibits

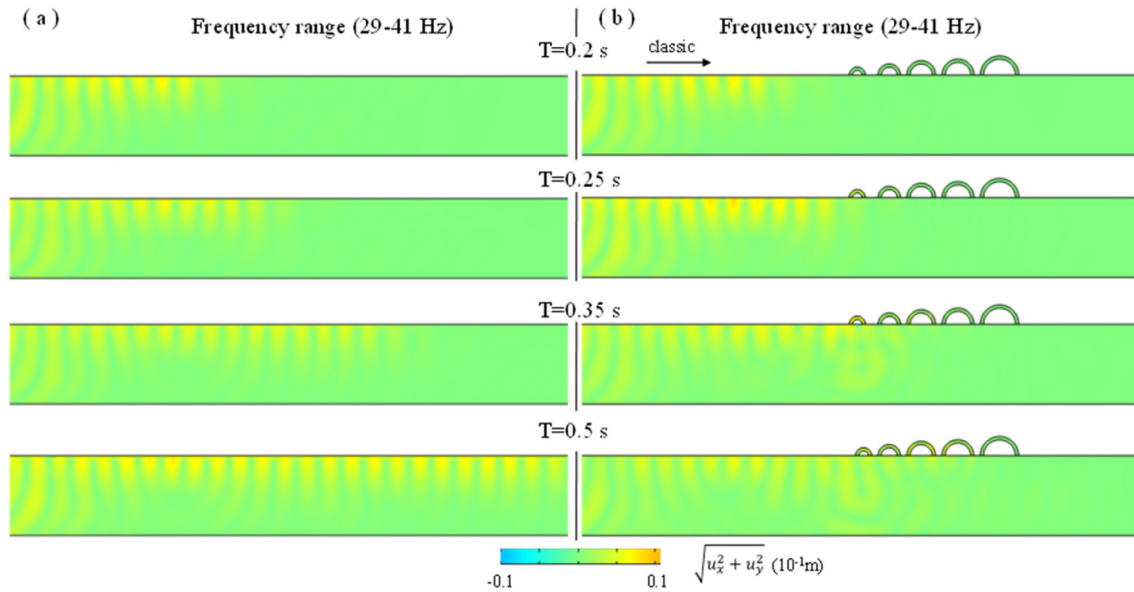


Fig. 5. Snapshots of Rayleigh wave propagating at different times, (a) without and (b) with the rainbow effect exhibited by gradient semicircle metasurfaces.

ultra-wide band gaps, the details of why the proposed metasurface exhibits ultra-wide band gap characteristics are explained. First of all, RSCM exhibits the wide band gap characteristics for Rayleigh waves above the lowest frequency controlled by the unit structure. On the other hand, the GSCM exhibits a wider band gap characteristic. Owing to that it is composed of unit structures with different sizes, and each unit structure obtains a specific band gap corresponding to a specific frequency range. GSCM combines the band gap characteristics of all unit structures, thus having the ultra-wide band gap characteristic. Details on the ultra-wide band gap characteristic of the proposed metasurface can be found in Supplementary Note 2 and Fig. 6. The investigations show the evidence of the ultra-wide band gap exhibited by the CSCM which combines RSCM and GSCM. To facilitate the comparison and verification of the ultra-wide band gap characteristics of CSCM, five frequency values are used as the simulation frequencies, i.e., 30 Hz and 70 Hz for the central frequencies of the band gap range of the unit structures and 15 Hz, 50 Hz and 90 Hz are the frequencies that cannot be controlled by each unit structure. Fig. 6 shows the snapshots of Rayleigh wave propagating at different frequencies with  $T = 0.5$  s. Of them, Fig. 6a, b describes the capability of CSCM to control the propagation of Rayleigh waves from two directions (see Supplementary Figs. 7 and 8), correspondingly, the displacement spectrum analysis results are shown in Fig. 6c, d. As shown in Fig. 6a, b, regardless of the central frequency and direction, the propagating Rayleigh waves can be well controlled by CSCM, which means the ability of CSCM to control the propagation of Rayleigh waves is not restricted by unit structure properties. In this regard, it can be clearly explained by three well-controlled Rayleigh waves with the central frequencies of 15 Hz, 50 Hz, and 90 Hz. Note that waves with these frequencies are hard to be controlled by each unit structures in CSCM. In addition, Fig. 6c, d further verify that CSCM performs well for the controlling of the surface amplitude response caused by Rayleigh waves propagating at different frequencies. It is worth noting that, as shown in Fig. 6c, d, as the frequency of Rayleigh wave increases, CSCM exhibits excellent control capabilities, which further proves the ultra-wide band gap characteristics of CSCM to a certain extent.

### 3. Practical engineering application-metabridge

The above analysis has shown that the capability of the proposed metasurface in controlling the propagation of seismic surface waves. To further explore its potentially rewarding applications, we extend the characteristics of the proposed metasurface to practical engineering applications. As an example, the application prospects of the proposed metasurface in bridge engineering was explored, which has always been the focus of research, for example, structural design, vibration mitigation, and fatigue life analysis [33–36]. The focus of this work is to apply the proposed metasurface to the bridge for achieving the advantages of vibration mitigation, thereby reducing the damage caused by the earthquake. Accordingly, we take the Jinsha river bridge in China (Fig. 7a) and the Dongjak bridge in Korea (Fig. 7b) as prototypes to construct the Metabridge, and then the finite element analysis was performed to verify the important role of the metabridge in controlling the propagation of seismic surface waves. Snapshots of Rayleigh waves ( $f = 15$  Hz) propagating at  $T = 0.5$  s is shown in Fig. 7c, d (see Supplementary Note 3 and Figs. 9–12), and the displacement spectrum analysis results are shown in Fig. 7e, f. As shown in Fig. 7c, d, one can find that there is wave propagation at the left end of the bridge (near the source), and almost no waves pass through the middle and right ends of the bridge, which shows that the propagating surface waves are well controlled. Furthermore, comparing the amplitude response curve of the bridge surface in Fig. 7e, f, one can find that the displacement of the bridge surface caused by vibration is well controlled, especially the metabridge with CSCM, which effectively realizes vibration isolation and protects the bridge from damage caused by earthquakes. Here, it is worth noting that there are two other advantages of the proposed metasurface that cannot be reflected in this bridge engineering case: (1) the simple semicircular structure significantly reducing the implementation complexity, and (2) the proposed metasurface can be flexibly applied to the design and maintenance stage of the bridge.

### 4. Conclusion and future work

In conclusion, we introduced a new type of metasurface for controlling the seismic surface waves, which can realize excellent performance in both low-frequency and wide band gap. The

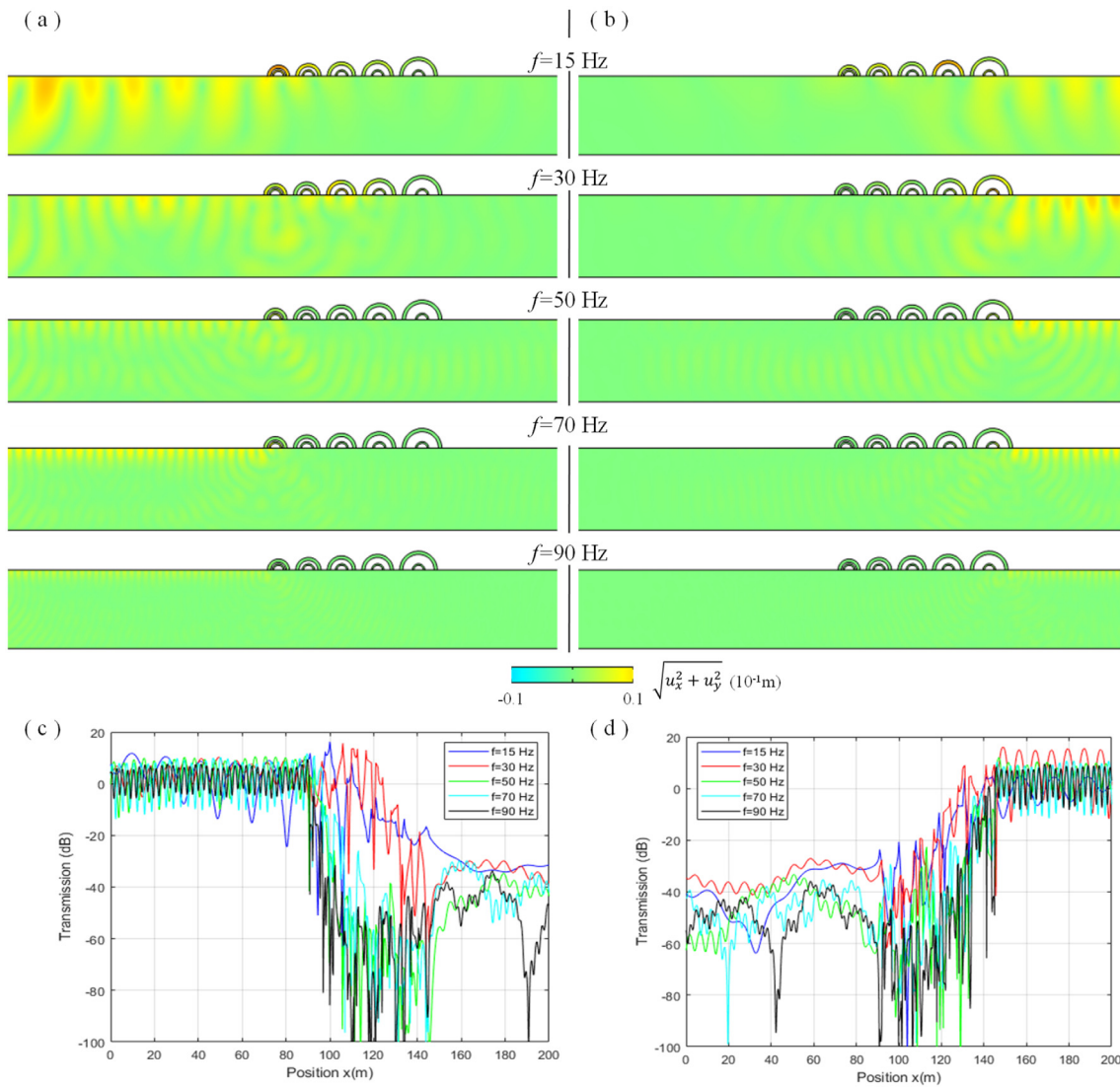


**Fig. 6.** Snapshots ( $T = 0.5$  s) of Rayleigh wave propagating at different frequencies, (a) and (b) Snapshots of Rayleigh waves propagating in two directions controlled by CSCM. (c) and (d) Amplitude response curve of ground surface caused by Rayleigh waves propagating at different frequencies controlled by CSCM.

proposed metasurface is designed by using an easy and simple method named the destructive interference, rather than the local resonance observed in previous methods. We demonstrate that even with simply designing the unit structure and arrange the unit structure in the form of periodicity by using functional gradient design and pattern combination, which results in hitherto better or even unprecedented control effect on the propagation of seismic surface waves. The mode-conversion characteristic of the proposed metasurface in controlling the propagation of Rayleigh waves is demonstrated. Then, the performance of the combined semicircular metasurfaces is shown for controlling the propagation of Rayleigh waves with both low-frequency and ultra-wide band gap. Moreover, the proposed metabridge can effectively protect the bridge from the damage of earthquakes. With the above characteristics and merits, we believe that the proposed metasurface provides new opportunities in practical engineering applications, such as seismology, civil engineering, and transportation engineering.

Future research to build upon this work will explore the control of shear wave propagation under uncertain conditions, for example, the control of wave propagation speed for structures whose mechanical properties change with time. In addition, the

influence of the connection properties between the metasurface and the ground is also worthy of further study.

#### Declaration of competing interest

The authors declare that they have no known competing financial interests or personal relationships that could have appeared to influence the work reported in this paper.

#### Acknowledgments

This work has been conducted during the first author's visit to Han Yang University. The financial supports were provided by the National Natural Science Foundation of China under Grant No. 51975589 and the Natural Science Foundation of Hunan Province, China under Grant No. 2018JJ3663, Fundamental Research Funds for the Central University of Central South University, China No. 2019zzts267, and the State Key Laboratory of Heavy-Duty AC Drive Electric Locomotive Systems Integration No. 2017ZJKF09. These sources of supports are gratefully acknowledged.

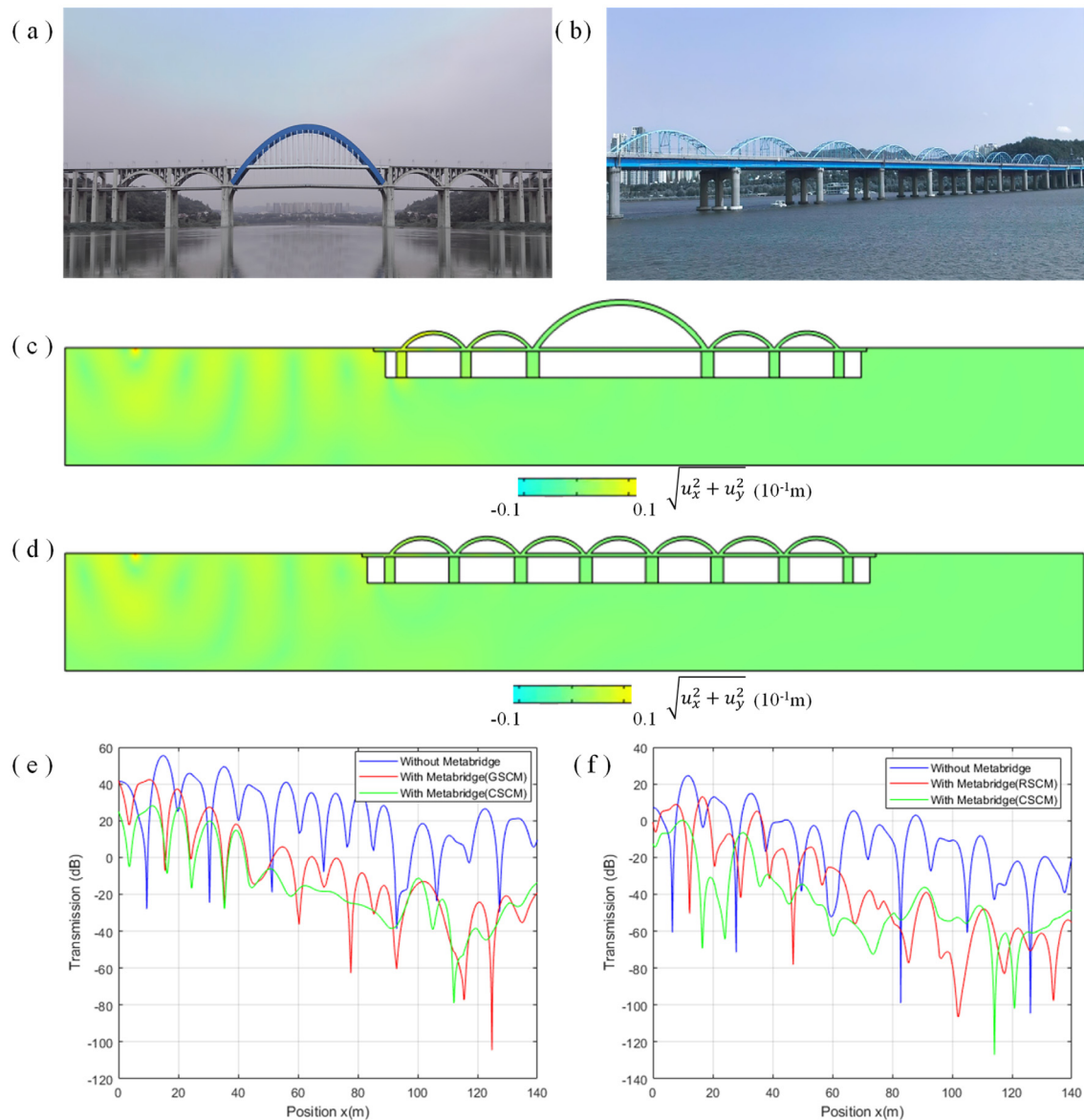


**Fig. 7.** The application of the proposed metasurfaces in bridge engineering (Metabridge). (a) Jinsha river bridge in China. (b) Dongjak bridge in Korea, (c) and (d) Snapshots of Rayleigh waves propagating controlled by Metabridge. (e) and (f) Amplitude response curve of bridge surface under control of Metabridge.

## Appendix A. Supplementary data

Supplementary material related to this article can be found online at <https://doi.org/10.1016/j.eml.2020.101018>. **Summary of Supplementary Files.** Details on the design and characteristics of the unit structure, see Supplementary Note 1; on the ultra-wide band gap characteristic of the proposed metasurface can be found in Supplementary Note 2; on the numerical simulation of the proposed metasurface in practical bridge engineering, see Supplementary Note 3. Moreover, Supplementary Figs. 1–12 describe the corresponding dynamic results of numerical simulation in our work.

## References

- [1] M.A.X. Born, Wave propagation in periodic structures, *Nature* 158 (1946) 926.
- [2] R.D. Woods, Screening of surface waves in soils, *J. Soil Mech. Found. Div.: Proc. Am. Soc. Civ. Eng.* 94 (1968) 951–979.
- [3] J. Aviles, F.J. Sanchezsesma, Piles as barriers for elastic waves, *J. Geotech. Eng.* 109 (1983) 1133–1146.
- [4] J. Li, L. Fok, X. Yin, G. Bartal, X. Zhang, Experimental demonstration of an acoustic magnifying hyperlens, *Nature Mater.* 8 (2009) 931–934.
- [5] L. Zigoneanu, B.-I. Popa, S.A. Cummer, Three-dimensional broadband omnidirectional acoustic ground cloak, *Nature Mater.* 13 (2014) 352–355.
- [6] T. Bückmann, M. Thiel, M. Kadic, R. Schittny, M. Wegener, An elastomechanical unfeelability cloak made of pentamode metamaterials, *Nature Commun.* 5 (2014) 4130, <http://dx.doi.org/10.1038/ncomms5130>.
- [7] S.H. Mousavi, A.B. Khanikaev, Z. Wang, Topologically protected elastic waves in phononic metamaterials, *Nature Commun.* 6 (2015) 8682, <http://dx.doi.org/10.1038/ncomms9682>.
- [8] S. Brûlé, S. Enoch, S. Guenneau, Emergence of seismic metamaterials: Current state and future perspectives, *Phys. Lett. A* 384 (2020) 126034.
- [9] D. Mu, H. Shu, L. Zhao, S. An, A review of research on seismic metamaterials, *Adv. Energy Mater.* (2020) 1901148.
- [10] S. Brule, E. Javelaud, S. Enoch, S. Guenneau, Experiments on seismic metamaterials: Molding surface waves, *Phys. Rev. Lett.* 112 (2014) 133901.
- [11] Y. Achaoui, et al., Clamped seismic metamaterials: Ultra-low frequency stop bands, *New J. Phys.* 19 (2017) 063022.
- [12] G.M. Alamo, J.D.R. Bordon, J.J. Aznarez, G. Lombaert, The effectiveness of a pile barrier for vibration transmission in a soil stratum over a rigid bedrock, *Comput. Geotech.* 110 (2019) 274–286.
- [13] S. Krödel, N. Thomé, C. Daraio, Wide band-gap seismic metastructures, *Extrem. Mech. Lett.* 4 (2015) 111–117.

- [14] Y. Achaoui, B. Ungureanu, S. Enoch, S. Brûlé, S. Guenneau, Seismic waves damping with arrays of inertial resonators, *Extrem. Mech. Lett.* 8 (2016) 30–37.
- [15] N. Yu, et al., Light propagation with phase discontinuities: Generalized laws of reflection and refraction, *Science* 334 (2011) 333–337.
- [16] X. Ni, A.V. Kildishev, V.M. Shalae, Metasurface holograms for visible light, *Nature Commun.* 4 (2013) 2807.
- [17] P. Genevet, et al., Ultra-thin plasmonic optical vortex plate based on phase discontinuities, *Appl. Phys. Lett.* 100 (2012) 013101.
- [18] D. Lin, P. Fan, E. Hasman, M.L. Brongersma, Dielectric gradient metasurface optical elements, *Science* 345 (2014) 298–302.
- [19] W. Yang, et al., All-dielectric metasurface for high-performance structural color, *Nature Commun.* 11 (2020) 1864.
- [20] M.S. Farajidana, et al., Compact folding surface spectrometer, *Nature Commun.* 9 (2018) 4196.
- [21] A.E. Cardin, et al., Surface-wave-assisted nonreciprocity in spatio-temporally modulated metasurfaces, *Nature Commun.* 11 (2020) 1–9.
- [22] Y. Yang, et al., Type-i hyperbolic metasurfaces for highly-squeezed designer polaritons with negative group velocity, *Nature Commun.* 10 (2019) 2002.
- [23] Y. Jin, R. Kumar, O. Poncelet, O. Mondainmonval, T. Brunet, Flat acoustics with soft gradient-index metasurfaces, *Nature Commun.* 10 (2019) 1–6.
- [24] A. Colombi, D.J. Colquitt, P. Roux, S. Guenneau, R.V. Craster, A seismic metamaterial: The resonant metawedge, *Sci. Rep.* 6 (2016) 27717.
- [25] A. Palermo, S. Krodel, A. Marzani, C. Daraio, Engineered metabarrier as shield from seismic surface waves, *Sci. Rep.* 6 (2016) 39356.
- [26] M. Addouche, M.A. Alleshaw, A. Elayouch, A. Khelif, Subwavelength waveguiding of surface phonons in pillars-based phononic crystal, *AIP Adv.* 4 (2014) 124303.
- [27] A. Maurel, J. Marigo, K. Pham, S. Guenneau, Conversion of love waves in a forest of trees, *Phys. Rev. B* 98 (2018).
- [28] A. Colombi, P. Roux, S. Guenneau, P. Gueguen, R.V. Craster, Forests as a natural seismic metamaterial: Rayleigh wave bandgaps induced by local resonances, *Sci. Rep.* 6 (2016) 19238.
- [29] J. Huang, Y. Liu, Y. Li, Trees as large-scale natural phononic crystals: Simulation and experimental verification, *Int. Soil Water Conserv. Res.* 7 (2019) 196–202.
- [30] M.A. Lethawe, M. Addouche, S. Benchabane, V. Laude, A. Khelif, Guidance of surface elastic waves along a linear chain of pillars, *AIP Adv.* 6 (2016) 121708.
- [31] A. Palermo, A. Marzani, Control of love waves by resonant metasurfaces, *Sci. Rep.* 8 (2018) 1–8.
- [32] X. Li, Y. Chen, X. Zhang, G. Huang, Shaping elastic wave mode conversion with a piezoelectric-based programmable meta-boundary, *Extrem. Mech. Lett.* 39 (2020) 100837.
- [33] A. Miyamoto, K. Kawamura, H. Nakamura, Bridge management system and maintenance optimization for existing bridges, *Comput.-Aided Civ. Infrastruct. Eng.* 15 (2000) 45–55.
- [34] A. Andersson, A. Oconnor, R. Karoumi, Passive and adaptive damping systems for vibration mitigation and increased fatigue service life of a tied arch railway bridge, *Computer-aided Civ. Infrastructure Eng.* 30 (2015) 748–757.
- [35] M. Baandrup, O. Sigmund, H. Polk, N. Aage, Closing the gap towards super-long suspension bridges using computational morphogenesis, *Nature Commun.* 11 (2020) 2735.
- [36] C. Zhang, C.C. Chang, M. Jamshidi, Concrete bridge surface damage detection using a single-stage detector, *Computer-aided Civ. and Infrastructure Eng.* 35 (2020) 389–409.